

STIS Target Acquisition

Steve Kraemer^{1,2}, Ron Downes³, Rocio Katsanis³, Mike Crenshaw¹, Melissa McGrath³, and Rich Robinson¹

Abstract. We describe the STIS autonomous target acquisition capabilities. We also present the results of dedicated tests executed as part of Cycle 7 calibration, following post-launch improvements to the STIS flight software. The residual pointing error from the acquisitions are < 0.5 CCD pixels, which is better than preflight estimates. Execution of peakups show clear improvement of target centering for slits of width $0''.1$ or smaller. These results may be used by Guest Observers in planning target acquisitions for their STIS programs.

1. Introduction

Target acquisition for STIS is required if an observer wishes to observe through one of the STIS spectroscopic slits. The method of target acquisition will depend on the type of target observed and the dimensions of the chosen spectroscopic slit. There are several types of autonomous STIS target acquisition, controlled by software executing in the STIS control section microprocessor. All modes of target acquisition will use images taken with one of the STIS detectors. Currently, only the STIS CCD is used for acquisition. The details of target acquisition are presented by Downes, Clampin, McGrath, & Shaw (1997). The paper presented here is intended to be a high level review of STIS target acquisition capability and a report of the results of acquisition tests executed during SMOV and as part of the Cycle 7 Calibration program.

2. Target Acquisition Modes

Autonomous target acquisition for STIS is divided into two modes: target location, which is used to place the target into a spectroscopic slit, and peakups, which are used to center the target within the slit. Both modes of acquisition execute the following set of functions: image taking, correction of the images for defects and cosmic ray hits, bias level subtraction, and the request to the HST main computer (NSSC-1) for correction maneuvers.

Two types of target locate are available to the GO's. The first is "point source" location. For a point source acquisition the STIS software will execute the following sequence:

1. After slew to STIS aperture, take two images of a $5'' \times 5''$ subarray, through one of the STIS imaging apertures. Perform corrections listed above. Find brightest 3×3 pixel "checkbox" and calculate target position via flux-weighted centroid.
2. Look up position of reference slit in on-board table. The reference slit is always the $0''.2 \times 0''.2$ slit.

¹Catholic University of America, NASA/Goddard Space Flight Center

²STIS IDT Member

³Space Telescope Science Institute

3. Request correction slew to place target where slit will project.
4. Retake image and find target as above.
5. Move slit wheel to reference slit. Illuminate slit with calibration lamp and find center of light pattern via threshold centroid (a flux-weighted centroid algorithm modified to eliminate errors due to non-uniform illumination).
6. Request final correction slew to center target in reference slit.
7. Slew to requested slit using aperture offset table (maintained in the ground system).

Images are taken in steps 1), 4) and 5). There will be no final confirmation image unless the GO includes it as a separate exposure.

The other type of target location is the “diffuse acquisition”. The steps are identical to those for a point source, but the GO may adjust the size of the “checkbox” to acquire a diffuse or extended source, and can either use a flux-weighted centroid or take the center pixel of the brightest checkbox (geometric-center) as the target location.

The other mode of autonomous acquisition is the peakup. The sequence will begin with the desired spectroscopic slit in place. The STIS software will execute a dwell scan, taking images at each point. The software will sum the flux in the subarray image at each dwell point. The software will determine the target location either by performing a flux-weighted centroid of the set of dwell point fluxes or, simply taking the dwell point with maximum flux. For a flux-weighted centroid, the minimum flux will be subtracted from each image, which effectively performs a bias subtraction and eliminates read noise. A correction slew is then requested and a confirmation image (the only one saved for downlink in this process) is taken.

The scan pattern used for the peak is tailored for the dimensions of the science slit. For example, a linear scan in the slit width direction is used for the long slits, linear scans in both dimensions for shorter slits, and spiral searches for the smallest echelle slits. Peakups can be executed in either undispersed light or, if there is sufficient flux, in dispersed light, but only in spectral modes that are available for the CCD. Finally, in addition to the peakup, a “peakdown” can be executed to center targets behind occulting bars. The method is essentially identical to that outlined above.

In the next section, we will review the results of target acquisition tests run to date; see also Katsanis et al. (1997) for early SMOV results.

3. The Results of On-orbit Target Acquisition Tests

The cycle 7 calibration program 7605, “TA checkout”, included tests of the basic target acquisition capabilities described in section II. Although these have all been demonstrated in earlier SMOV programs, 7605 was executed after a set of flight software modifications were installed. These modifications included the elimination of a set of bad columns in CCD subarray images (an artifact of the readout software) from the area checked for the target, the revised bias/darknoise subtraction algorithm for peakups mentioned earlier, and a change in the NSSC-1 software to avoid truncation of commanded offsets, which had affected the dwell scan pattern used in peakups. Therefore, the results of 7605 are the best way to assess the accuracy of STIS autonomous target acquisition.

Three point source acquisitions were executed. Two on a bright target (G93-48) and one on a faint target (the BL Lac PKS1255-316). The accuracy of the results were determined by measuring the target position in a confirmation image taken through the 6"x6" aperture, and a corresponding correction was made to determine the position of the target within the slit. As noted above, GO's will not get confirmation images unless they add a

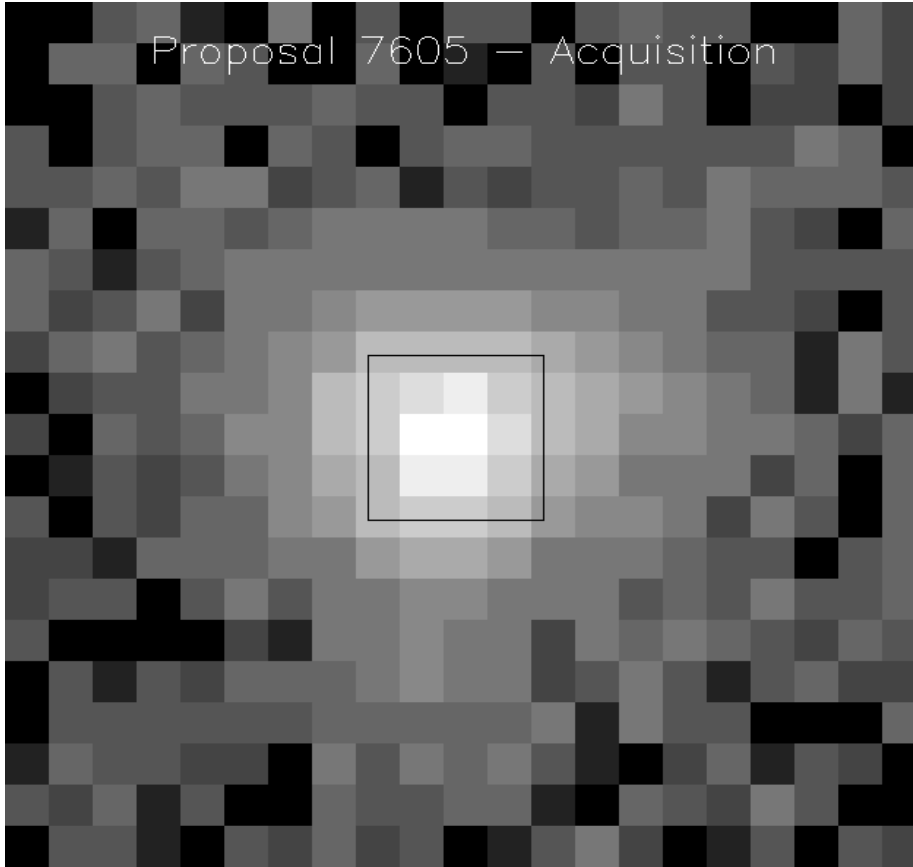


Figure 1. Confirmation image after acquisition of the target into a $0''.2 \times 0''.2$ slit. The position of the slit is drawn on the image. First order dispersion is in the horizontal, or "X", direction.

separate exposure after the acquisition. The results are as follows. Positions are given in CCD detector coordinates.

1) For the faint target acq (PKS1255-316):

total counts in brightest checkbox:	641	
	X	Y
position of reference aperture:	534.4	517.0
position of target in slit: (corrected for 6x6 aperture)	534.3	517.0
error in acquisition:	0.1	0.0 (pixels)
	0.005	0.0 (arcseconds)

The result of this acquisition are shown in Figure 1, in which we have superimposed the outline of the slit on the confirmation image taken in the $6'' \times 6''$ aperture. As one can see, this pictorial demonstration confirms the analysis shown above.

2) For the bright target acq (G93-48):

total counts in brightest checkbox:	9082	
	X	Y
position of reference aperture:	535.0	517.3
position of target in slit: (corrected for 6x6 aperture)	535.0	517.5
error in acquisition:	0.0	-0.2 (pixels)
	0.0	-0.01 (arcseconds)

3) For the bright target acq, second visit (G93-48):

total counts in brightest checkbox:	9018	
	X	Y
position of reference aperture:	534.8	516.8
position of target in slit: (corrected for 6x6 aperture)	534.6	516.6
error in acquisition:	0.2	0.2 (pixels)
	0.010	0.010 (arcseconds)

Two diffuse source acquisitions were executed. These both had the galaxy RXJ1347.5 as the target and were taken with exposure times of 250 and 30 seconds, respectively, to see how the acquisition would work at the nominal S/N and with low counts. Both used the flux-weighted centroid algorithm. Note that the accuracy of diffuse acquisitions tends to be lower than for the point source, due to the flatter image profile of the target and size of the checkbox used. The results were as follows.

1) At the nominal exposure time:

total counts in brightest checkbox:	5040	
	X	Y
position of reference aperture:	533.4	516.3
position of target in slit: (corrected for 6x6 aperture)	534.7	516.9
error in acquisition:	-1.3	-0.6 (pixels)
	-0.066	-0.031 (arcseconds)

2) At low counts. Note that this had failed earlier in SMOV due to the bright column problem mentioned above.

total counts in brightest checkbox:	465	
	X	Y
position of reference aperture:	533.4	516.3
position of target in slit: (corrected for 6x6 aperture)	534.7	517.6
error in acquisition:	-1.3	-1.3 (pixels)
	-0.065	-0.065 (arcseconds)

Several different peakups were executed as part of this program. The error in the final pointing can be estimated by fitting a gaussian to the set of data points, determining the position of maximum flux and finding where the flux in the confirmation image would fall. The difference gives the error.

Some examples:

1) target - PKS1255-316

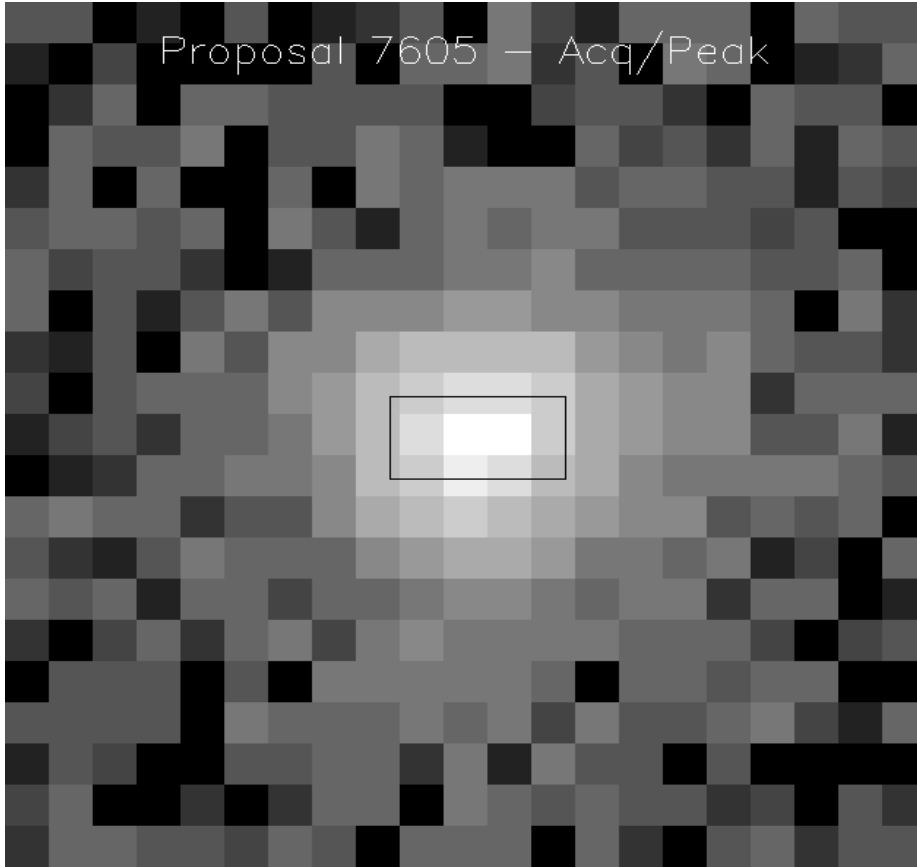


Figure 2. Confirmation image after acquisition/peakup of the target into a $0''.1 \times 0''.2$ slit. The position of the slit is drawn on the image.

- peakup in $52'' \times 0''.1$ slit, in undispersed light, using 5 step scan with stepsize = 75 milliarcsec.
- initial flux (after target locate) = 4437
- flux after centering = 5086
- error, from comparison to gaussian fit = 0.016 pixels ($0.0008''$)

2) target - PKS1255-316

- peakup in $0''.1 \times 0''.2$ slit, in undispersed light, using 5 step scan with stepsize = 75 milliarcsec.
- initial flux (after target locate) = 5079
- flux after centering = 5165
- error, from comparison to gaussian fit = 0.082 pixels ($0.004''$)

In Figure 2, we show the outline of the $0''.1 \times 0''.2$ slit superimposed on the confirmation image. Comparison with Figure 1 gives a qualitative measure of the improvement in pointing offered by the peakup mode.

Another way to measure the accuracy of the peakup is to measure the flux of the target through the slit and compare it to the flux in a wider aperture, taking the relative throughput into account. This was done for 7605 by comparing the flux of the target in the peakup confirmation image to the flux in a post-acq image taken through the $6'' \times 6''$ aperture. The predicted relative throughputs are given in Robinson (1997). For example, the results of two peakups of the star GS93-48 in undispersed light were as follows: for a peakup in the $0''.1 \times 0''.2$ slit, the throughput ratio was 0.66, compared to a predicted ratio of 0.60, while for a peakup in the $0''.1 \times 0''.09$ slit, the ratio was 0.64, compared to a prediction of 0.49. Although this measurement is sensitive to the amount of background included (we used a 20×20 pixel area in both cases), it does show that the peakup can be used to maximize throughput, and helps confirm the analysis done using a Gaussian fit.

Peakups may also be executed in dispersed light. In the three cases that were run in this mode during the execution of 7605, the fluxes in the confirmation images were equal to those at the end of the target locate, within Poisson statistical error. We confirm that the peakup did not degrade the pointing accuracy. Since, we did not have confirmation images taken through wider slits to get a measure of the relative throughput, we cannot tell if improved centering were achieved. It should be noted that before the flight software upgrade that made the bias subtraction more robust, this mode routinely failed.

In SMOV proposal 7073, we demonstrated the capability to center a target behind an occulting bar, using a “peakdown” routine. The results are shown in Figures 3 and 4. Qualitatively, we can state that the method worked as planned, and the target is well centered behind the occulting bar.

Finally, it does not appear that peakups are effective if the slit width is $\geq 0''.2$. Early in SMOV, peakups in slits of this width did improve pointing, but the improvement was due to the elimination of a systematic offset related to the refractive properties of filters used during the target locate. Once the systematic error was eliminated, the target locate became sufficiently accurate to abrogate the need for a peakup in $0''.2$ wide slits. Note that including the peakup for these slits does not significantly change the centering, either for the better or the worse. It is, rather, unnecessary.

4. Conclusions

STIS possess accurate and robust autonomous target acquisition capabilities. Target locate and peakup processes have been demonstrated for a variety of targets and optical modes, and the results show that the instrument can be used to center targets in small spectroscopic slits required for high resolution spectroscopy. The improvements in the flight software made during SMOV have addressed early problems with image quality that made the acquisition of faint targets less reliable.

An observer can decide which mode of target acquisition is required to support their science, based on observing mode and type of target. The target locate process, both for point and extended sources, is highly accurate and may suffice for most types of STIS science. For example, for slits of width $0''.2$ or greater, it will be unnecessary to perform a peakup, since the locate will already provide the maximum centering accuracy. It should also be noted that point source acquisitions may work as well for extended targets, as long as the light profile possesses a central peak. The diffuse locate is preferable for targets whose surface brightness varies unevenly. An observer may determine the best mode to use by using the STScI target acquisition software available on-line (see STIS site at <http://www.stsci.edu>).

There are still improvements to be made for STIS target acquisition. New methods for the flagging of hot pixels that may affect an acquisition are being discussed, and will be included during cycle 7. Although these will be transparent for the observer, they will result in fewer acquisition failures, particularly for faint targets.

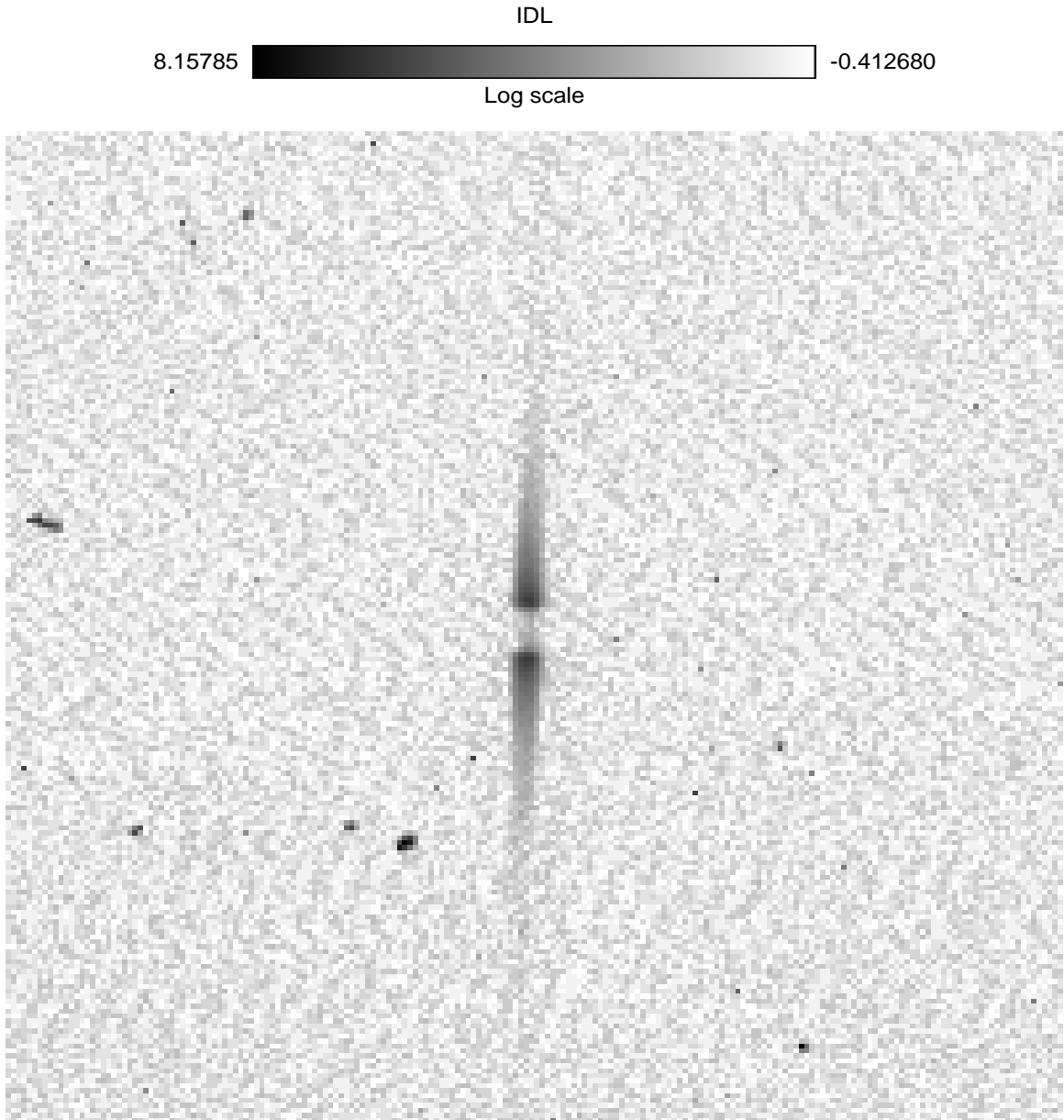


Figure 3. STIS CCD (undispersed) image of a star after acquisition and peak-down into into an occulting bar in a 52"x0".2 slit.

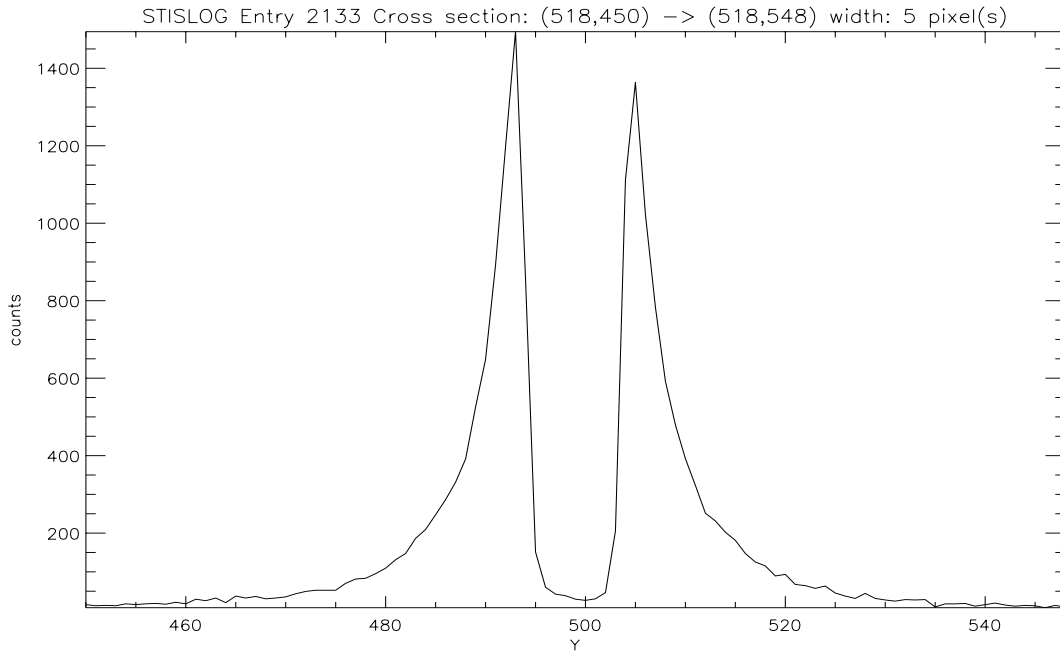


Figure 4. Plot along the length of the slit (in the “Y” direction) in Figure 3.

Also, the results of peakups in slits of size $0''.2$ show no pointing improvement, and therefore they should be deleted in cases where they are included as part of the default method.

References

- Downes, R., Clampin, M. McGrath, M. & Shaw, R. 1997, Instrument Science Report STIS 97-03 (Baltimore:STScI)
- Katsanis, R. Downes, R., Hartig, G., & Kraemer, S. 1997, Instrument Science Report STIS 97-12 (Baltimore:STScI)
- Robinson, R. 1997, Quick-Look Post-Launch STIS Calibration Report, No. 44